Are Piezoelectric–Electromagnetic Hybrid Energy Harvesting Systems Beneficial?

Binh Duc Truong, Cuong Phu Le, and Shad Roundy

***Abstract*—The primary objective of this work is to investigate the performance of a hybrid energy harvesting system consisting of piezoelectric and electromagnetic transducers. We first show that a single–mechanism generator with negligible electrical losses, referred to as an electrically–lossless harvester, can reach the theoretical power bound regardless of the coupling strength between the mechanical and electrical domains, which renders the use of hybrid systems unnecessary. For a more realistic analysis, the electrically parasitic losses are then taken into account. We introduce effective figures of merit for the piezoelectric and electromagnetic generators that combine transducer coupling and resistive losses. The maximum output power of single–transducer and hybrid systems are determined analytically, expressed as functions of effective figures of merit. We find that there is no benefit to utilizing a hybrid system if one of the two, or both, effective figures of merit exceeds a threshold of $\mathcal{M}^* \approx 2.17$. We also derive the narrow conditions under which a resonant hybrid harvester system with multiple transduction mechanisms can outperform its counterpart which uses a single energy conversion. In order to provide a comprehensive assessment of the configurations considered, we analyze the relationships between optimizing system efficiency and maximizing output power. We reveal that the two problems generally yield different solutions. However, for a hybrid structure, these objectives result in a unique solution when the effective figures of merit of the two transductions are equal. This is a distinctive property of a hybrid system compared to a single–mechanism device.**

***Index Terms*—Power Optimization, Energy Harvesting, Wireless Power Transfer, Multi–mechanism System**

I. Introduction

ENERGY harvesting technology has grown rapidly in the last two decades as an alternative to conventional power sources for low–power electronics. It is becoming a key enabling technology for various applications, ranging from structural health monitoring to wearable and implantable devices, and for the future internet of things [1]–[4]. Energy harvesting systems capture energy from ambient sources and convert them into electricity by employing various transduction technologies, such as, thermoelectric, pyroelectric, piezoelectric, electromagnetic, magnetoelectric, and triboelectric. Until recently, an energy harvester typically utilized a single energy conversion mechanism. However, hybrid energy harvesters are attracting more and more attention [5]–[8]. Hybrid systems can be classified into two categories, multi–source energy harvesters and single–source harvesters with multiple mechanisms. In this work, we narrow our focus on the latter.

Kinetic energy harvester is one of the most, if not the most, investigated topics of energy harvesting due to the availability of environmental vibration and the diversity in energy transformation techniques [9]. Alongside thermal generator, vibration harvester also plays a dominant role in hybrid energy harvesting [8]. The three common combinations in a vibrational hybrid energy harvesting system are piezoelectric–electromagnetic, piezoelectric–triboelectric, and triboelectric–electromagnetic. We choose a configuration that includes piezoelectric and electromagnetic transducers as an example of the study. However, similar analysis methodologies can be extended and generalized for the remaining architectures under linear operation due to the similarities in their mathematical models.

Hybrid energy harvesters are expected to improve space utilization efficiency and increase total output power [10]–[13]. However, previous studies on hybrid systems have not considered the parasitic losses of piezoelectric and electromagnetic transducers simultaneously. While this reduces the complexity of the problem, it also limits the accuracy of the results. Later, we will show that these electrically–lossless generators are always able to reach the theoretical power bound regardless of whether the transducer is weakly or strongly coupled. This finding raises a question about the need for a hybrid architecture. Motivated by that, we account for both loss factors to better model a realistic hybrid device and seek

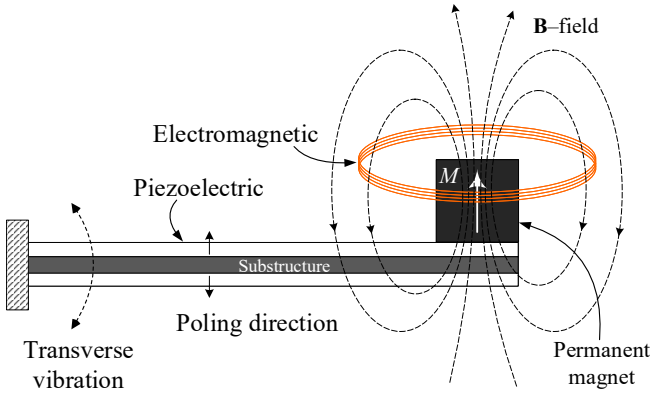

Fig. 1: Schematic of a piezoelectric–electromagnetic hybrid system.

Manuscript received Month Day, Year; revised Month Day, Year; accepted Month Day, Year. Date of publication Month Day, Year; date of current version Month Day, Year. Corresponding authors: Binh Duc Truong, email: drtruong@umich.edu.

Binh Duc Truong is with the Department of Mechanical Engineering, University of Michigan, Ann Arbor, MI 48109, USA. Cuong Phu Le is with the Department of Electronic Systems, Norwegian University of Science and Technology (NTNU), Trondheim, Norway. Shad Roundy is with the Department of Mechanical Engineering, University of Utah, Salt Lake City, UT 84112, USA.

to comprehend the system performance in a more rigorous manner. Furthermore, it is unclear under what circumstances, if any, introducing more than one transduction mechanism is beneficial. Addressing this concern is the central objective of the paper.

We consider a common and single mass for the transducers and linear loading. We limit our analysis to situations where the mass displacement is unrestricted (which may not applicable for small–scale devices such as MEMS/NEMS energy harvesters with proof mass vibrating in the transverse direction). In the following sections, we derive analytical solutions to the maximum power delivered to the load for both single–mechanism generators and hybrid energy harvesters, utilizing circuit theory and impedance matching techniques. We formulate an inequality as a criterion for comparing their performance. The results obtained by solving the inequality suggest that the conditions under which a hybrid system outperforms are rather narrow, raising skepticism about the necessity of employing multiple transduction mechanisms in practice. The approach we use here is applicable to other similar energy harvesting or wireless power transfer systems, such as devices reported in [14]–[16].

While incorporating well–established findings regarding electrically–lossless harvesters, single–mechanism systems, and the physical power bound, we aim to provide a cohesive perspective by considering these results from a unified standpoint. However, the primary contributions of this paper revolve around analyzing the power and efficiency performance of a hybrid configuration and comparing it to conventional systems that employ a single transduction method.

II. Piezoelectric–Electromagnetic Hybrid Systems: Mathematical Model

An example structure of a hybrid energy harvesting system composed of piezoelectric and electromagnetic transducers is illustrated in Figure 1. A permanent magnet is mounted at the tip of a cantilever that is a bimorph piezoelectric composite beam. Two piezoelectric layers are poled in opposite directions and connected in series. A pickup coil is placed in proximity to the magnet mass, forming an electromagnetic generator. Under an external excitation, the mass vibrates in the transverse direction, and its kinetic energy can be converted to electricity simultaneously through the piezoelectric effects and Faraday's law of induction. It is important to note that the excitation can be vibration or magnetic fields. In the latter case, the interactions between the magnet and the **B**–field or the magnetic flux gradient create a moment or a force acting on the resonator. Therefore, although we focus on energy harvesting systems, the structure under consideration can represent three different device types, a vibration energy harvester, a magnetic energy harvester, and a receiver for a low–frequency wireless power transfer system [14]–[16].

The system in Figure 1 can be described by a linear three–port model whose equivalent circuit is shown in Figure 2 [17]. m, b, and K_0 are the effective mass, mechanical damping coefficient, and mechanical stiffness. The equivalent drive force has the form of $F = F_0 \cos(\omega t)$ where ω is the operating angular frequency. Ψ and Γ are the electromagnetic and electromechanical transduction factors. L_1 and C_0 are the inductance of the pickup coil and the equivalent capacitance of the piezoelectric composite. The model also includes inevitable parasitic losses of the two transducers (i.e., conductive losses of the coil and dielectric losses of piezoelectric material). These losses are characterized by two resistances, one in series with the coil inductance and the other in parallel with the piezoelectric capacitance, denoted as R_1 and R_0, respectively. In typically idealized models of electrically–lossless generators, the resistances R_0 and R_1 are omitted based on the assumption that losses due to parasitic resistance are negligible. The effects of the parasitic capacitance in parallel with L_1 are disregarded in the frequencies of interest. The analysis in this paper applies to linear vibration energy harvesters driven by harmonic vibration. The performance evaluation of non–linear energy harvesting systems and harvesters driven by shock or colored and white noise vibrations is beyond the scope of this paper.

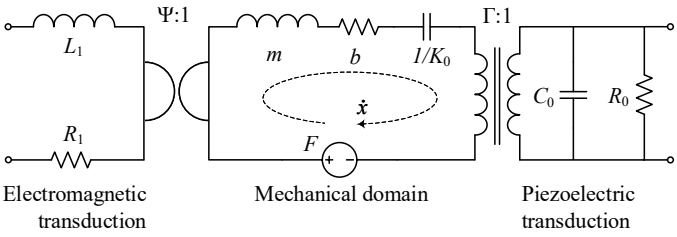

Fig. 2: Equivalent circuit of linear three–port model.

III. Electrically–Lossless Generators

In this Section, we revisit some well–known results presented in previous works for electrically–lossless linear energy harvesters that utilize one transduction mechanism. However, we consider these results from the perspective of the impedance matching method [18], instead of the widely–used gradient descent approach [19], [20]. We then show that, theoretically, such a harvester can always reach the power bound with any positive coupling strength, therefore, obviating the need for a hybrid system with multiple mechanisms.

Hybrid energy harvesting systems simplify to single–mechanism harvesters if only one transduction of energy conversion of the hybrid systems is active when the output terminals of the other one are open (for the electromagnetic transduction) or shorted (for the piezoelectric transduction). In the following analysis, the electromagnetic transducer is taken as an example, but the results hold for both types of generators.

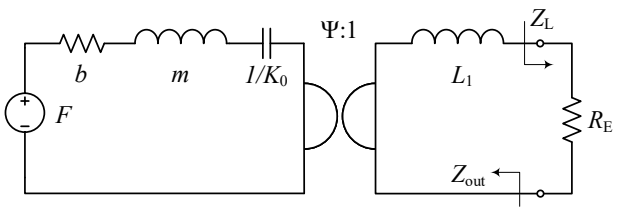

Fig. 3: Equivalent circuit model of an electrically–lossless electromagnetic harvester with a purely resistive load.

Figure 3 shows an idealized model of an electromagnetic energy harvester without electrical losses. A load resistance $R_{\rm E}$ is connected to the electrical port for the sake of simplification. This model yields two distinct regimes for the maximum output power generated at the load [21], [22], determined by the resonator figure of merit $M_{\rm E} = \Delta K_{\rm E}/(\omega b)$, where $K_{\rm E} = K_0 + \Delta K_{\rm E}$ and $\Delta K_{\rm E} = \Psi^2/L_1$. For $M_{\rm E} \leq 2$, the optimal load and frequency are given by

$$\begin{aligned} R_{\rm E} &= \omega L_1, \\ \omega^2 &= \frac{K_0 + \Delta K_{\rm E}/2}{m}. \end{aligned} \tag{1}$$

The corresponding maximum obtained power is

$$P_{\rm E} = \frac{F_0^2}{8b}\frac{8M_{\rm E}}{(M_{\rm E}+2)^2}. \tag{2}$$

For $M_{\rm E} \geq 2$, the optimal choices of load and frequency are determined by the following equations

$$\begin{aligned} \omega\tau_{\rm E} &= \left(M_{\rm E} \pm \sqrt{M_{\rm E}^2 - 4}\right)/2, \\ m\omega^2 &= K_0 + \Delta K_{\rm E}\frac{M_{\rm E} \pm \sqrt{M_{\rm E}^2-4}}{2M_{\rm E}} \end{aligned} \tag{3}$$

where $\tau_{\rm E} = L_1/R_{\rm E}$ is an electrical time constant associated with the load. This solution always leads to the output power

$$P_{\rm E} = \frac{F_0^2}{8b}. \tag{4}$$

When the resonator figure of merit reaches a critical value of $M_{\rm E} = 2$, a transition between the two regimes occurs. At this threshold, expression (2) coincides with (4). These results were derived using the gradient descent method, and we can now analyze them from an impedance–matching point of view to possibly gain further understanding.

The maximum possible output power delivered to the load can be found by applying network theory [23], [24]. In Figure 3, $Z_{\rm out}$ represents the output impedance seen from the load, and $Z_{\rm L}$ is a general expression of the load impedance. In this case, the real and imaginary parts of $Z_{\rm L}$ are, respectively, $\Re\{Z_{\rm L}\} = R_{\rm E}$ and $\Im\{Z_{\rm L}\} = 0$. Two different impedance matching conditions can be considered separately as follows

$$|Z_{\rm out}| = R_{\rm E}, \tag{5}$$

$$Z_{\rm out} = Z_{\rm L}^*. \tag{6}$$

The latter condition is equivalent to requiring that the real part of $Z_{\rm out}$ is equal to $R_{\rm E}$ and the imaginary part is canceled out.

The expression of the output impedance $Z_{\rm out}$ in Figure 3, its real and imaginary parts and amplitude squared are

$$\begin{aligned} Z_{\rm out} &= j\omega L_1 + \frac{\Psi^2}{j(\omega m - K_0/\omega) + b}, \\ \Re\{Z_{\rm out}\} &= \frac{\Psi^2 b}{(\omega m - K_0/\omega)^2 + b^2}, \\ \Im\{Z_{\rm out}\} &= \omega L_1 + \frac{\Psi^2(K_0 - m\,\omega^2)}{\omega\left((\omega m - K_0/\omega)^2 + b^2\right)}, \\ |Z_{\rm out}|^2 &= \omega^2 L_1^2 + \frac{\Psi^2\omega^2(\Psi^2 - 2L_1 m\omega^2 + 2K_0 L_1)}{K_0^2 - \omega^2(2K_0 m - b^2) + m^2\,\omega^4}. \end{aligned}$$

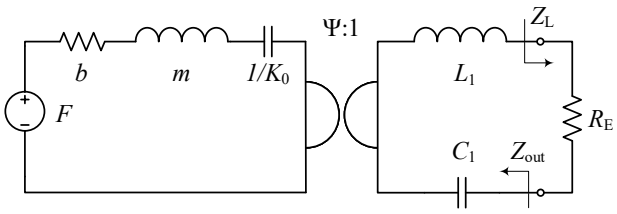

Fig. 4: An electrically–lossless electromagnetic harvester with a resistive load connected in series with an external capacitor.

Substituting ω^2 in (1) into $|Z_{\rm out}|^2$ and simplifying, we get

$$\begin{aligned} |Z_{\rm out}|^2 &= \frac{L_1\left(\Psi^2 + 2K_0L_1\right)}{2m} = \frac{L_1^2\left(\Delta K_{\rm E}/2 + K_0\right)}{m} \\ &= (\omega L_1)^2 = R_{\rm E}^2, \end{aligned}$$

or equivalently, $|Z_{\rm out}| = R_{\rm E}$. Furthermore, with solution (1), we also find that $\Im\{Z_{\rm out}\} = 0$ if and only if $M_{\rm E} = 2$. Such a special case aligns with the strong coupling regime to be investigated in the next paragraph. In most scenarios (i.e., $M_{\rm E} < 2$), $\Im\{Z_{\rm out}\} \neq 0$ and it is impossible to satisfy condition (6). These analyses indicate that, generally, tuning the load and frequency in the weak coupling regime can be considered as matching the load resistance with only the amplitude of the output impedance.

In the same manner, based on the relationships in (3), we find that

$$\begin{aligned} \Im\{Z_{\rm out}\} &= \omega L_1\left(1 - \frac{2M_{\rm E}\left(M_{\rm E} \pm \sqrt{M_{\rm E}^2-4}\right)}{\left(M_{\rm E} \pm \sqrt{M_{\rm E}^2-4}\right)^2 + 4}\right) = 0, \\ \Re\{Z_{\rm out}\} &= \omega L_1 \frac{2}{M_{\rm E} \pm \sqrt{M_{\rm E}^2-4}} = R_{\rm E}, \end{aligned}$$

which gives $Z_{\rm out} = Z_{\rm L}^*$. Therefore, in the strong coupling regime, simultaneously optimizing the load and frequency is equivalent to perfectly match the load and the output impedance.

We notice that if the condition (6) is fulfilled, the load and output impedance are fully matched, which enables the electromagnetic generator to provide the largest possible power, as shown in (4). Otherwise, if condition (5) holds, only the amplitude of the load impedance matches that of the output impedance, while the phases are still different. As a result of this impedance mismatch, the output power in (2) always being less than or equal to that in (4). In summary, to achieve the maximum output power, it is necessary for the load and output impedance to be precisely matched.

Moreover, previous studies of two–port energy harvesters have shown that by employing (6) as a sufficient condition to identify the optimal load and frequency, theoretical power limit can be achieved [25]. Therefore, equation (6) can be considered as the necessary and sufficient condition to reach the maximum possible power. However, condition (6) can only be met when $M_{\rm E} \geq 2$. Is this a strict requirement on the physics of the energy harvesting system, or just a limitation of the resistive–loaded model under consideration? We seek to address this concern in the following investigations.

Let us consider an electrically–lossless transducer without constraining the load impedance to resistance. In particular, we

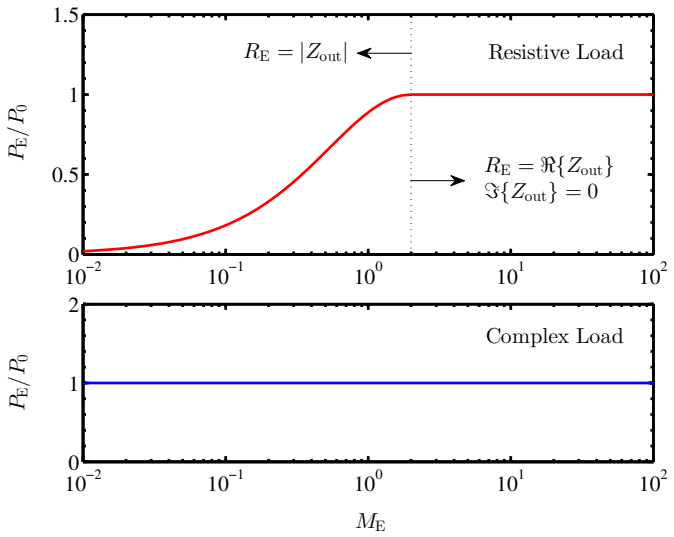

Fig. 5: Comparison of output power between a purely resistive load and a complex load for electrically–lossless models. The latter case is equivalent to forming a resonator in the electrical domain by employing an external capacitor. Here, we define $P_0 = F_0^2/(8b)$.

add an external capacitor C_1 in series with both R_E and L_1, as depicted in Figure 4. This configuration can be viewed as incorporating a general complex load impedance or forming a resonator in the electrical domain. The output impedance seen from the load now becomes

$$Z_{out} = j\left(\omega L_1 - \frac{1}{\omega C_1}\right) + \frac{\Psi^2}{j(\omega m - K_0/\omega) + b}.$$

By operating the system at the mechanical resonance frequency and carefully choosing the added capacitance such that $\omega = \omega_0 = \sqrt{K_0/m} = 1/\sqrt{L_1 C_1}$, and matching the load resistance with the real part of the output impedance, $R_E = \Psi^2/b$, the output power is then

$$P_E = \frac{1}{2}\left(\frac{F_0}{b + \Psi^2/R_E}\Psi\right)^2 \frac{1}{R_E} = \frac{1}{2}\frac{F_0^2}{(2b)^2} b = \frac{F_0^2}{8b},$$

which is identical to (4). More importantly, this result is derived without any assumption or requirement on the coupling strength (or the resonator figure of merit) as long as they are positive. This finding is in contrast with the previous result presented in the literature, for instance, [20], [26], [27], where $M_E \geq 2$ is a necessary condition to attain the maximum possible output power. It means that, *this well–known argument only holds true for a harvester model in which the load impedance is limited to resistance.* A similar conclusion was reported in [28], [29] for piezoelectric energy harvesters where the dielectric losses are negligible. A summary of the maximum output power of two models, without and with a resonator formed in the electrical domain, is demonstrated in Figure 5.

The presented analysis shows that, in principle, the harvester can deliver the maximum power to the load regardless of the degree of coupling between the mechanical and electrical domains. Therefore, in the absence of electrical losses, utilizing multiple energy conversion mechanisms does not provide benefits in terms of power. However, intrinsic losses are inevitable in many practical scenarios, particularly in electromagnetic energy harvesters, where the inductive coil resistance cannot be neglected. Exploring the performance of a more realistic system that includes these unavoidable factors is therefore of greater interest and is the main aim of the following Sections. Moreover, the impedance matching approach is proven powerful and is an appropriate alternative to the gradient descent method for finding the maximum power. Especially when the system becomes more complicated, the impedance matching technique is valuable in reducing the calculation complexity in an analytical fashion and is therefore employed as the primary means in further explorations.

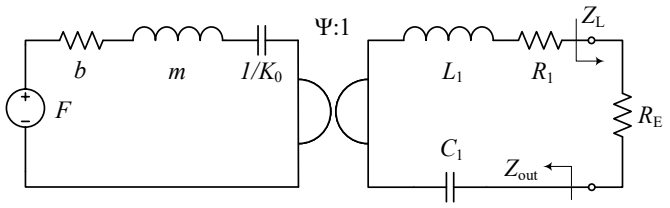

Fig. 6: Equivalent circuit model for electromagnetic transducer that includes resistive losses.

IV. Power Optimization for Each Single Transducer

In this section, we extend the analysis presented in Section III to account for electrical losses in harvesters that utilize a single transduction mechanism. The equivalent circuit model for the case where only electromagnetic transduction is active is shown in Figure 6, which includes the coil resistance R_1. Similar to the last part of Section III, one approach to realize the impedance matching is to form a resonator in the electrical domain by incorporating an external capacitor C_1 in series with the harvester coil L_1. The output impedance Z_{out} is then

$$Z_{out} = j\left(\omega L_1 - \frac{1}{\omega C_1}\right) + R_1 + \frac{\Psi^2}{j(\omega m - K_0/\omega) + b}.$$

The imaginary parts of Z_{out} in both mechanical and electrical domains are eliminated by choosing the appropriate operating frequency and added capacitance, in particular, $\omega = \sqrt{K_0/m} = 1/\sqrt{L_1 C_1}$. As a consequence, condition $\Im\{Z_{out}\} = 0$ holds.

Solving the condition $\Re\{Z_{out}\} = R_E$ yields

$$\tau_E = \frac{\tau_1}{1 + \mathcal{M}_E} \tag{7}$$

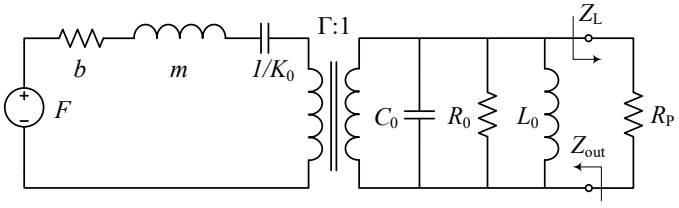

Fig. 7: Equivalent circuit for piezoelectric transducer, taking parasitic losses into account.

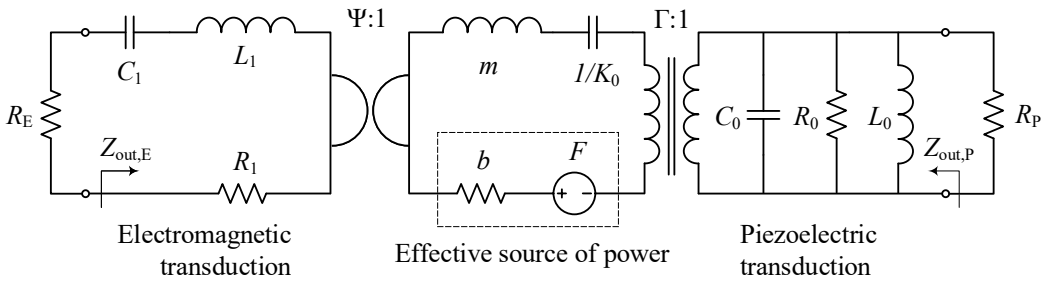

Fig. 8: Equivalent circuit model for a piezoelectric–electromagnetic hybrid system.

where $\tau_1 = L_1/R_1$ and $\mathcal{M}_\mathrm{E} = \Psi^2/(bR_1)$. The corresponding output power is

$$P_\mathrm{E} = \frac{F_0^2}{8b}\frac{\mathcal{M}_\mathrm{E}}{\mathcal{M}_\mathrm{E}+1}. \tag{8}$$

By definition, the squared electromagnetic coupling coefficient is given by $k_\mathrm{E}^2 = \Psi^2/(K_\mathrm{E}L_1)$. The expedient coupling coefficient (or the generalized coupling coefficient) is defined as $k_\mathrm{e,E}^2 = k_\mathrm{E}^2/(1-k_\mathrm{E}^2)$. Thus, we arrive at $\Psi^2 = k_\mathrm{e,E}^2 K_0 L_1 = k_\mathrm{e,E}^2 m\omega_0^2 L_1$. Introducing the mechanical quality factor and the coil quality factor at resonance frequency ω_0, $Q_0 = \omega_0 m/b$ and $Q_\mathrm{L} = \omega_0 L_1/R_1$, we can write

$$\mathcal{M}_\mathrm{E} = \frac{\Psi^2}{bR_1} = k_\mathrm{e,E}^2\left(\frac{m\omega_0}{b}\right)\left(\frac{\omega_0 L_1}{R_1}\right) = k_\mathrm{e,E}^2 Q_0 Q_\mathrm{L}.$$

In Section III, the resonator figure of merit of an electromagnetic transducer is defined in a general form as $M_\mathrm{E} = \Delta K_\mathrm{E}/(\omega b)$. At resonance, $\omega = \omega_0$, the parameter M_E can be written as $M_\mathrm{E} = \Psi^2/(\omega_0 bL_1) = k_\mathrm{e,E}^2 K_0/(\omega_0 b) = k_\mathrm{e,E}^2(\omega_0 m/b) = k_\mathrm{e,E}^2 Q_0$. Accordingly, it follows that $\mathcal{M}_\mathrm{E} = M_\mathrm{E}Q_\mathrm{L}$. Therefore, $\mathcal{M}_\mathrm{E}$ can be interpreted as an *effective figure of merit* of the electromagnetic generator, taking into account the presence of the parasitic resistance R_1.

For a piezoelectric harvester, its equivalent circuit model is depicted in Figure 7. The result obtained for electromagnetic generator in (8) is applicable to piezoelectric transducer. In particular,

$$P_\mathrm{P} = \frac{F_0^2}{8b}\frac{\mathcal{M}_\mathrm{P}}{\mathcal{M}_\mathrm{P}+1} \tag{9}$$

where $\mathcal{M}_\mathrm{P} = \Gamma^2 R_0/b$. In analogy to the electromagnetic energy harvester, the piezoelectric generator has relevant parameters that can be defined as follows. The electrical quality factor associated with dissipation due to losses is $Q_\mathrm{C} = \omega_0 R_0 C_0$. The electromechanical coupling coefficient is $k_\mathrm{P}^2 = \Gamma^2/(K_\mathrm{P}C_0)$, where $K_\mathrm{P} = \Delta K_\mathrm{P} + K_0$ and $\Delta K_\mathrm{P} = \Gamma^2/C_0$. The corresponding generalized coupling coefficient is $k_\mathrm{e,P}^2 = k_\mathrm{P}^2/(1-k_\mathrm{P}^2)$. The piezoelectric–resonator figure of merit is $M_\mathrm{P} = \Delta K_\mathrm{P}/(\omega b)$, and at resonance, $M_\mathrm{P} = k_\mathrm{e,P}^2 Q_0$. We can also write $\mathcal{M}_\mathrm{P} = k_\mathrm{e,P}^2 Q_0 Q_\mathrm{C} = M_\mathrm{P}Q_\mathrm{C}$.

In summary, the maximum possible power that the electromagnetic and piezoelectric generators can provide is given by (8) and (9), respectively. It is worth noting that an alternative approach by means of network theory and reflected impedance yields the same limit on power, as detailed in Appendix A.

We find that $P_\mathrm{E} \geq P_\mathrm{P}$ if and only if $\mathcal{M}_\mathrm{E} \geq \mathcal{M}_\mathrm{P}$, or equivalently, $\Psi/\Gamma \geq \sqrt{R_0 R_1}$. Furthermore, in contrast to the electrically–lossless two–port model discussed in Section III, there is no threshold for the effective figure of merit (beyond which power saturates). In this case, the power levels given in (8) and (9) always increase with $\mathcal{M}_\mathrm{E}$ and $\mathcal{M}_\mathrm{P}$, respectively. With the electrical losses taken into account, P_P and P_E are always less than $F_0^2/(8b)$, and the larger the effective figures of merit $\mathcal{M}_\mathrm{E}$ and $\mathcal{M}_\mathrm{P}$ are, the closer P_P and P_E are to the theoretical power bound of $F_0^2/(8b)$. At the limit, $P_\mathrm{E,P} \to F_0^2/(8b)$ when $\mathcal{M}_\mathrm{E,P} \to +\infty$, which can also be used to approximate the output power of a harvester with low electrical losses (i.e., $R_1 \to 0$ or $R_0 \to +\infty$).

There are various possible pathways to increase the effective figures of merit $\mathcal{M}_\mathrm{E}$ and $\mathcal{M}_\mathrm{P}$, for example, reducing the mechanical damping, designing (and operating) a system with a higher resonance frequency at a given coupling coefficient, or minimizing the electrically parasitic losses. The first method depends on packaging technologies, such as fabricating a device in a vacuum or creating a rigid anchor to prevent thermal losses at clamping points [27], [30]. Meanwhile, the harvester resonance frequency is usually designed depending on the frequency of the environmental vibration. For an electromagnetic energy harvester, the number of turns of the coil is proportional to both inductance and resistance [31]. Although increasing the number of turns has little effect on the coil quality factor Q_L, it significantly enhances the electrodynamic transduction factor (or equivalent, the coupling coefficient) [32], thereby increasing $\mathcal{M}_\mathrm{E}$. For a piezoelectric transducer, it is difficult to distinguish the electrical from mechanical and piezoelectric losses [33]. However, advanced piezoelectric materials typically have small and negligible electrical losses [34].

While this section aims to derive the power limit without practical constraints, which allows us to incorporate an external capacitor or inductor to form a resonator, some authors may be interested in how the system performs with only the resistive load. In order to provide a more complete picture, in Appendix B, we explore a maximum output power by optimizing the load and frequency using the gradient descent method. The results suggest that, even without relying on a resonator, it is possible to achieve power levels close to the maximum power described in (8) and (9) by simultaneously optimizing the load and frequency or even with an optimal load resistance at resonance.

V. Power Optimization for a Hybrid System

We now consider a general case in which both generators operate simultaneously. The equivalent circuit model for this case is presented Figure 8. The impedance matching theory is utilized to derive the output power of each mechanism, and their summation yields the total maximum power, $P_{\rm T}$. The output impedance $Z_{\rm out,P}$ and $Z_{\rm out,E}$ seen by the piezoelectric and electromagnetic generators are given by

$$\begin{aligned} Z_{\rm out,P}^{-1} &= R_0^{-1} + (j\omega L_0)^{-1} + j\omega C_0 \\ &\quad + \Gamma^2\Big(b + j\omega m + K_0/(j\omega) \\ &\quad + \Psi^2\big(R_{\rm E} + R_1 + j\omega L_1 + (j\omega C_1)^{-1}\big)^{-1}\Big)^{-1}, \\ Z_{\rm out,E} &= R_1 + j\omega L_1 + (j\omega C_1)^{-1} \\ &\quad + \Psi^2\Big(b + j\omega m + K_0/(j\omega) \\ &\quad + \Gamma^2\big(R_{\rm P}^{-1} + R_0^{-1} + (j\omega L_0)^{-1} + j\omega C_0\big)^{-1}\Big)^{-1}. \end{aligned}$$

Following the approach presented in Section IV, the drive frequency ω and the external components L_0 and C_1 are chosen such that $\omega = \sqrt{K_0/m} = 1/\sqrt{L_0C_0} = 1/\sqrt{L_1C_1}$. This choice makes $\Im\{Z_{\rm out,E}\} = \Im\{Z_{\rm out,P}\} = 0$.

The optimal loads are then obtained by matching to the real part of the corresponding output impedances. Setting $R_{\rm E} = \Re\{Z_{\rm out,E}\}$ and $R_{\rm P} = \Re\{Z_{\rm out,P}\}$, we get

$$\frac{1}{R_{\rm P}} = \frac{1}{R_0} + \frac{\Gamma^2}{b + \Psi^2/(R_1 + R_{\rm E})}, \tag{10}$$

$$R_{\rm E} = R_1 + \frac{\Psi^2}{b + \Gamma^2 R_0 R_{\rm P}/(R_0 + R_{\rm P})} \tag{11}$$

These two equations are coupled, in which each equation contains both variable of interest $R_{\rm P}$ and $R_{\rm E}$. The positive solutions to $R_{\rm P}$ and $R_{\rm E}$ are

$$R_{\rm P} = R_0\sqrt{\frac{b(\Psi^2 + R_1 b)}{(R_0\Gamma^2 + b)(R_0R_1\Gamma^2 + R_1 b + \Psi^2)}},$$

$$R_{\rm E} = \sqrt{\frac{(\Psi^2 + R_1 b)(R_0R_1\Gamma^2 + R_1 b + \Psi^2)}{b(R_0\Gamma^2 + b)}}.$$

In some cases, it might be convenient to express these solutions in terms of dimensionless parameters, which show the direct connections between time constants and effective figures of merit, as follows,

$$\tau_{\rm P} = \tau_0\sqrt{\frac{\mathcal{M}_{\rm E} + 1}{(\mathcal{M}_{\rm P} + 1)(\mathcal{M}_{\rm P} + \mathcal{M}_{\rm E} + 1)}}, \tag{12}$$

$$\tau_{\rm E} = \tau_1\sqrt{\frac{\mathcal{M}_{\rm P} + 1}{(\mathcal{M}_{\rm E} + 1)(\mathcal{M}_{\rm E} + \mathcal{M}_{\rm P} + 1)}} \tag{13}$$

where the time constants of the piezoelectric resonator are given by $\tau_{\rm P} = R_{\rm P}C_0$ and $\tau_0 = R_0C_0$, and $\tau_{\rm E}$ and τ_1 are defined in Section III. Methods to calculate the output power of the single–transduction harvester models in Sections III and IV are well–known and straightforward. However, determining the total generated power of a hybrid system is somewhat more complicated, and a procedure to do that is discussed next.

The complex velocity amplitude of the proof mass is

$$\mathcal{V}_{\rm m} = \frac{F_0}{b + Z}$$

where Z represents the input impedance seen from the effective source of power formed by $\{F, b\}$, and is given by

$$\begin{aligned} Z &= j\omega m + K_0/(j\omega) \\ &\quad + \Gamma^2\big(R_0^{-1} + R_{\rm P}^{-1} + (j\omega L_0)^{-1} + j\omega C_0\big)^{-1} \\ &\quad + \Psi^2/\big(R_1 + R_{\rm E} + j\omega L_1 + (j\omega C_1)^{-1}\big). \end{aligned} \tag{14}$$

The voltages across the load resistance $R_{\rm E}$ and $R_{\rm P}$ and the corresponding output power are

$$\begin{aligned} V_{\rm E} &= \frac{\mathcal{V}_{\rm m}\Psi}{R_1 + R_{\rm E} + j\omega L_1 + 1/(j\omega C_1)}R_{\rm E}, \\ V_{\rm P} &= \Big\{F_0 - \big[j\omega m + K_0/(j\omega) + b \\ &\quad + \Psi^2/\Big(R_1 + R_{\rm E} + j\omega L_1 + (j\omega C_1)^{-1}\Big)\big]\,\mathcal{V}_{\rm m}\Big\}\Big/\Gamma \\ P_{\rm E} &= \frac{1}{2}\frac{|V_{\rm E}|^2}{R_{\rm E}},\ P_{\rm P} = \frac{1}{2}\frac{|V_{\rm P}|^2}{R_{\rm P}}. \end{aligned}$$

These equations provide general forms of $V_{\rm E}, V_{\rm P}, P_{\rm E}$ and $P_{\rm P}$ that are applicable to any physical set of system parameters.

Let us first proceed with the electromagnetic transduction. Due to the resonance condition that we choose, all the imaginary parts cancel each other. $V_{\rm E}$ then simplifies to

$$V_{\rm E} = \frac{R_{\rm E}}{R_{\rm E} + R_1}\frac{\Psi F_0}{b + \Re\{Z\}}$$

where $\Re\{Z\} = \Gamma^2/\big(R_0^{-1} + R_{\rm P}^{-1}\big) + \Psi^2/(R_1 + R_{\rm E})$. As $R_{\rm E}$ is solution of equation (11), we have that $\Gamma^2/\big(R_0^{-1} + R_{\rm P}^{-1}\big) = \Psi^2/(R_{\rm E} - R_1) - b$, thus, $b + \Re\{Z\} = 2\Psi^2R_{\rm E}/(R_{\rm E}^2 - R_1^2)$. The quantities $V_{\rm E}$ and $P_{\rm E}$ then become

$$V_{\rm E} = \frac{F_0(R_{\rm E} - R_1)}{2\Psi}, \tag{15}$$

$$\begin{aligned} P_{\rm E} &= \frac{F_0^2}{8b}\frac{(R_{\rm E} - R_1)^2}{\dfrac{\Psi^2}{bR_1}R_1R_{\rm E}} = \frac{F_0^2}{8b}\frac{(R_{\rm E}/R_1 - 1)^2}{\dfrac{\Psi^2}{bR_1}\dfrac{R_{\rm E}}{R_1}} \\ &= \frac{F_0^2}{8b}\frac{(\tau_1/\tau_{\rm E} - 1)^2}{\mathcal{M}_{\rm E}\,\tau_1/\tau_{\rm E}}. \end{aligned} \tag{16}$$

Substituting (13) into (16), the output power of the electromagnetic transduction mechanism is

$$P_{\rm E} = \frac{F_0^2}{8b}\frac{\big(\sqrt{\mathcal{M}_{\rm E} + 1}\sqrt{\mathcal{M}_{\rm E} + \mathcal{M}_{\rm P} + 1} - \sqrt{\mathcal{M}_{\rm P} + 1}\big)^2}{\mathcal{M}_{\rm E}\sqrt{\mathcal{M}_{\rm E} + 1}\sqrt{\mathcal{M}_{\rm P} + 1}\sqrt{\mathcal{M}_{\rm E} + \mathcal{M}_{\rm P} + 1}},$$

Following the same procedure, the output voltage and power of the piezoelectric transduction mechanism are

$$\begin{aligned} V_{\rm P} &= \frac{F_0(1 - R_{\rm P}/R_0)}{2\Gamma}, \\ P_{\rm P} &= \frac{F_0^2}{8b}\frac{1}{\Gamma^2R_0/b}\frac{(1 - R_{\rm P}/R_0)^2}{R_{\rm P}/R_0}, \\ &= \frac{F_0^2}{8b}\frac{1}{\mathcal{M}_{\rm P}}\frac{(1 - \tau_{\rm P}/\tau_0)^2}{\tau_{\rm P}/\tau_0} \end{aligned}$$

Thus, we obtain

$$P_{\mathrm{P}} = \frac{F_0^2}{8b} \frac{\left(\sqrt{\mathcal{M}_{\mathrm{P}}+1}\sqrt{\mathcal{M}_{\mathrm{P}}+\mathcal{M}_{\mathrm{E}}+1} - \sqrt{\mathcal{M}_{\mathrm{E}}+1}\right)^2}{\mathcal{M}_{\mathrm{P}}\sqrt{\mathcal{M}_{\mathrm{P}}+1}\sqrt{\mathcal{M}_{\mathrm{E}}+1}\sqrt{\mathcal{M}_{\mathrm{P}}+\mathcal{M}_{\mathrm{E}}+1}},$$

and the total output power is

$$\begin{aligned} P_{\mathrm{T}} &= \frac{F_0^2}{4b}\left(\frac{1}{\mathcal{M}_{\mathrm{P}}}+\frac{1}{\mathcal{M}_{\mathrm{E}}}\right)\left[\frac{\sqrt{\mathcal{M}_{\mathrm{P}}+1}\sqrt{\mathcal{M}_{\mathrm{E}}+1}}{\sqrt{\mathcal{M}_{\mathrm{P}}+\mathcal{M}_{\mathrm{E}}+1}} - 1\right] \\ &= \frac{F_0^2}{8b}\frac{2(\mathcal{M}_{\mathrm{P}}+\mathcal{M}_{\mathrm{E}})}{1+\mathcal{M}_{\mathrm{P}}+\mathcal{M}_{\mathrm{E}}+ \sqrt{(\mathcal{M}_{\mathrm{P}}+1)(\mathcal{M}_{\mathrm{E}}+1)(\mathcal{M}_{\mathrm{P}}+\mathcal{M}_{\mathrm{E}}+1)}}. \end{aligned} \tag{17}$$

The inequality $\sqrt{(\mathcal{M}_{\mathrm{P}}+1)(\mathcal{M}_{\mathrm{E}}+1)(\mathcal{M}_{\mathrm{P}}+\mathcal{M}_{\mathrm{E}}+1)} > (\mathcal{M}_{\mathrm{P}}+\mathcal{M}_{\mathrm{E}})$ holds for all positive values of $\mathcal{M}_{\mathrm{P}}$ and $\mathcal{M}_{\mathrm{E}}$. Therefore, the total power P_{T} is always less than $F_0^2/(8b)$ (the largest possible power that the effective power source can provide). This result is consistent with circuit theory. In addition, (17) reduces to (8) or (9) if only either the electromagnetic or piezoelectric generator is active. In particular,

$$\lim_{\mathcal{M}_{\mathrm{E}}\to 0} P_{\mathrm{T}} = \frac{F_0^2}{8b}\frac{\mathcal{M}_{\mathrm{P}}}{\mathcal{M}_{\mathrm{P}}+1},$$
$$\lim_{\mathcal{M}_{\mathrm{P}}\to 0} P_{\mathrm{T}} = \frac{F_0^2}{8b}\frac{\mathcal{M}_{\mathrm{E}}}{\mathcal{M}_{\mathrm{E}}+1},$$

which verifies the consistency of (8), (9), and (17).

The method of forming resonators by connecting the capacitor and inductor in series or parallel used in Sections III, IV and V is a convenient mathematical approach to determine the maximum output power. However, the required capacitance or inductance might be too large to be feasible, especially for low–frequency systems. Therefore, in practice, simultaneously optimizing the load resistance and the operating frequency could be of more interest. Smart power electronic interfaces such as the synchronized switch harvesting on inductor (SSHI) and the synchronous electric charge extraction (SECE) can also be utilized as alternatives [29], [35], [36]. In the next section, we aim to identify circumstances in which a single–mechanism or hybrid system is preferable to the other.

VI. When is utilizing a multi-mechanism system helpful?

A multi–mechanism system is preferable over a single transduction configuration in terms of power if and only if the total output power of the hybrid structure (employing both transductions) is greater than those of each counterpart system that only uses a single mechanism. The relevant conditions are solved based on the inequality formed by the power expressions obtained from the two cases, which reads

$$P_{\mathrm{T}} \geq \max\{P_{\mathrm{E}}, P_{\mathrm{P}}\} \tag{18}$$

where P_{E}, P_{P}, and P_{T} are given in (8), (9), and (17), respectively. We retain the equality condition in (18) to clarify the mathematical solutions where the equality is met. Without loss of generality, we first examine the inequalities

$$\begin{cases} P_{\mathrm{T}} \geq P_{\mathrm{E}}, \\ \mathcal{M}_{\mathrm{E}} \geq \mathcal{M}_{\mathrm{P}}. \end{cases} \tag{19}$$

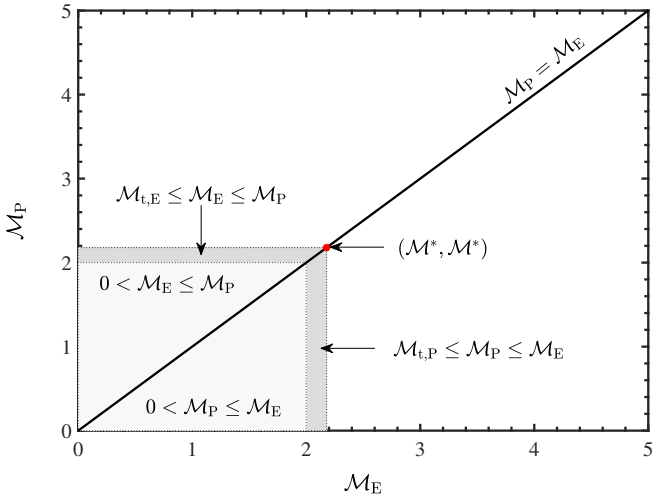

Fig. 9: Conditions of $\mathcal{M}_{\mathrm{E}}$ and $\mathcal{M}_{\mathrm{P}}$ under which a hybrid energy harvesting system is useful. The solution is constrained by a square with a diagonal formed by the origin $(0,0)$ and point $(\mathcal{M}^*, \mathcal{M}^*)$. Outside this region, a hybrid configuration does not yield any benefit.

With both $\mathcal{M}_{\mathrm{E}}$ and $\mathcal{M}_{\mathrm{P}}$ being positive, (19) reduces to

$$\begin{cases} \mathcal{M}_{\mathrm{E}}(\mathcal{M}_{\mathrm{E}}^2 - 4)(\mathcal{M}_{\mathrm{E}}+\mathcal{M}_{\mathrm{P}}+1) - 4\mathcal{M}_{\mathrm{P}} \leq 0, \\ 0 < \mathcal{M}_{\mathrm{P}} \leq \mathcal{M}_{\mathrm{E}}. \end{cases} \tag{20}$$

Solutions to (20) are summarized as follows

$$\begin{cases} 0 < \mathcal{M}_{\mathrm{P}} \leq \mathcal{M}_{\mathrm{E}} \ \forall \mathcal{M}_{\mathrm{E}} \in (0, 2], \\ \mathcal{M}_{\mathrm{t,P}} \leq \mathcal{M}_{\mathrm{P}} \leq \mathcal{M}_{\mathrm{E}} \forall\, \mathcal{M}_{\mathrm{E}} \in (2, \mathcal{M}^*) \end{cases} \tag{21}$$

where

$$\mathcal{M}_{\mathrm{t,P}} = \frac{\mathcal{M}_{\mathrm{E}}(\mathcal{M}_{\mathrm{E}}+1)(\mathcal{M}_{\mathrm{E}}-2)(\mathcal{M}_{\mathrm{E}}+2)}{-\mathcal{M}_{\mathrm{E}}^3 + 4\mathcal{M}_{\mathrm{E}} + 4},$$

$$\mathcal{M}^* = \frac{1}{6}\left(\sqrt[3]{359 - 12\sqrt{78}} + \sqrt[3]{359 + 12\sqrt{78}} - 1\right) \approx 2.17.$$

We note that the inequality $0 < \mathcal{M}_{\mathrm{t,P}} < 2 < \mathcal{M}_{\mathrm{E}}$ holds for all $\mathcal{M}_{\mathrm{E}} \in (2, \mathcal{M}^*)$. Due to the symmetry in the roles of $\mathcal{M}_{\mathrm{E}}$ and $\mathcal{M}_{\mathrm{P}}$, solution (21) holds when exchanging $\mathcal{M}_{\mathrm{P}}$ for $\mathcal{M}_{\mathrm{E}}$.

In summary, if any of $\mathcal{M}_{\mathrm{P}}$ or $\mathcal{M}_{\mathrm{E}}$ exceeds $\mathcal{M}^*$, a hybrid system does not provide any benefit since P_{T} is always less than P_{P} or P_{E} (i.e., inequality (18) is not satisfied). On the contrary, a hybrid harvester is beneficial for the following cases. Case I, with any $0 < \mathcal{M}_{\mathrm{i}} \leq \mathcal{M}_{\mathrm{j}}$ for all $0 < \mathcal{M}_{\mathrm{j}} \leq 2$. And Case II, when $\mathcal{M}_{\mathrm{i}}$ is equal to or greater than $\mathcal{M}_{\mathrm{t,i}}$ and equal to or less than $\mathcal{M}_{\mathrm{j}}$ for all $2 < \mathcal{M}_{\mathrm{j}} < \mathcal{M}^*$, where $(\mathrm{i}, \mathrm{j}) = \{(\mathrm{P}, \mathrm{E}) \vee (\mathrm{E}, \mathrm{P})\}$ and $\mathcal{M}_{\mathrm{t,i}}$ is a function of $\mathcal{M}_{\mathrm{j}}$. The solutions are divided by different domains as shown in Figure 9. It is straightforward that the parameter space under which a hybrid device outperforms a single–mechanism transducer is much smaller than the physical possibilities where $\mathcal{M}_{\mathrm{P}}$ and $\mathcal{M}_{\mathrm{E}}$ can take on any positive value.

A visualization of the findings is presented in Figure 10. We note that $P_{\mathrm{P}} = P_{\mathrm{E}}$ when $\mathcal{M}_{\mathrm{P}} = \mathcal{M}_{\mathrm{E}}$, and Figure 10 remains unchanged if the two quantities $\mathcal{M}_{\mathrm{P}}$ and $\mathcal{M}_{\mathrm{E}}$ are swapped. Let us consider the case when the effective figure of merit of

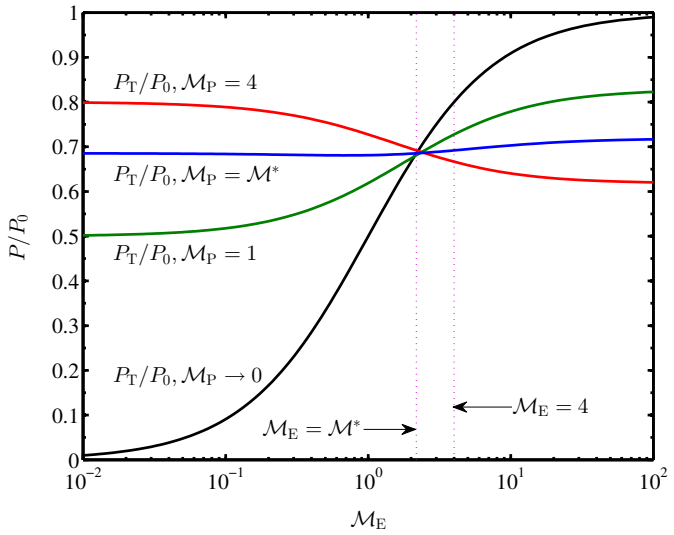

Fig. 10: Comparison between the output power of single– and multiple–transduction systems. $P_{\rm T}$ is given by (17) and $P_0 = F_0^2/(8b)$.

the piezoelectric transducer is fixed at $\mathcal{M}_{\rm P} = 4 > \mathcal{M}^*$ as an example (i.e., red solid line in the figure). If the harvester only contains a single piezoelectric transducer, we have that $P_{\rm P}/P_0 = 4/5 = 0.8$, where $P_0 = F_0^2/(8b)$, due to (9). The maximum output power of a hybrid system $P_{\rm T}$, given by (17), is always less than $P_{\rm P}$. $P_{\rm T} \to P_{\rm P}$ only if $\mathcal{M}_{\rm E} \to 0$, and $P_{\rm T}$ decreases with the increase of $\mathcal{M}_{\rm E}$. Therefore, a hybrid system is not preferable to a single transduction device under this circumstance.

In general, if a harvester cannot provide sufficiently strong coupling with a single transduction mechanism (i.e., given size and material constraints), a hybrid system can be considered an alternative to increasing the coupling. Otherwise, introducing another transduction mechanism adds loss that counteracts the increased coupling. We show the exact values for a figure of merit, for which coupling is a constituent part, above which a hybrid system is counterproductive.

VII. Discussion: On the Efficiency of a Single–Mechanism and Hybrid Energy Harvesting Systems

The efficiency of an energy harvesting system may also be an important quantity for consideration [27], [37]–[41]. As a conventional definition, efficiency is the ratio between the power delivered to the load and the power input to the harvester, $\eta = P_{\rm L}/P_{\rm in}$. Intuitively, maximizing the output power seems to be equivalent to optimizing efficiency. This conclusion holds for a wireless power transfer system, in which a power source is limited by its impedance and the voltage it can provide. In this case, the global optimal point of maximizing transferred power and efficiency coincide with a unique solution [42]. However, this property may no longer hold for an energy harvesting system where the inertial force acting on the proof mass is assumed to be able to provide the mass with an unlimited velocity. In particular, optimizing output power and efficiency are different scenarios for a harvester, which has been proven for electrically–lossless transducers [27]. This Section is devoted to extending our understanding of the relationships between maximum power and efficiency to single– and multi–mechanism harvesters that take electrically parasitic losses into account. We explore the corresponding efficiency at maximum power condition and the output power associated with the maximum efficiency condition. These examinations can provide additional insights into the trade–off between maximum power and efficiency for energy harvesting systems, complementing our previous analysis of the three models under consideration in this paper.

The input power of an energy harvesting system is defined as

$$P_{\rm in} = \frac{F_0^2}{2}\frac{\Re\{Z_{\rm in}\}}{|Z_{\rm in}|^2}$$

where $Z_{\rm in}$ is the input impedance including both mechanical and electrical impedance. For a hybrid structure, $Z_{\rm in} = b + Z$, where Z is given by (14). For a harvester utilizing only one transduction mechanism, either term contributed by piezoelectric or electromagnetic generator in (14) vanishes. In the idealized case where the electrical losses are neglected, Z is further simplified with $R_0 = 0$ and $R_1 \to +\infty$. We focus on three circumstances, similar to Sections III, IV, and V. Although electromagnetic energy harvesting systems are analyzed as an example, the results hold for their piezoelectric counterparts.

A. Electrically–lossless energy harvester

It has been shown that when the ideal two–port harvester in Figure 4 reaches its maximum output power of $F_0^2/(8b)$, the energy conversion efficiency is $\eta|_{\max\{P_{\rm E}\}} = 1/2$. We now investigate the maximum efficiency of this electrically–lossless resonant generator. Similar to the analysis in the previous Sections, the operating frequency is chosen at resonance, $\omega = \omega_0 = \sqrt{K_0/m}$, resulting in

$$P_{\rm E} = \frac{1}{2}\frac{F_0^2}{(b + \Psi^2/R_{\rm E})^2}\frac{\Psi^2}{R_{\rm E}},$$
$$P_{\rm in} = \frac{F_0^2}{2b}\left(1 + \frac{\Psi^2}{bR_{\rm E}}\right)^{-1},$$
$$\eta = \frac{\Psi^2}{bR_{\rm E} + \Psi^2}.$$

Since $\mathrm{d}\eta/\,\mathrm{d}R_{\rm E} = -\Psi^2 b/(bR_{\rm E} + \Psi^2)^2$ is negative, η always increases with the decrease of $R_{\rm E}$, and $\eta \to 1$ if $R_{\rm E} \to 0$. This can be interpreted that when the load resistance is close to the short–circuited condition, the output power is nearly identical to the input power, however, both are approaching zero and no useful power is obtained. For an ideal, lossless harvester, maximizing the system efficiency is not an appropriate choice.

B. Single–mechanism energy harvesters with electrical parasitic losses

For the system investigated in Section IV, when the maximum power conditions are satisfied, the input power and

efficiency are

$$P_{\rm in}|_{\max\{P_{\rm E}\}} = \frac{F_0^2}{4b}\frac{\mathcal{M}_{\rm E}+2}{\mathcal{M}_{\rm E}+1},$$
$$\eta|_{\max\{P_{\rm E}\}} = \frac{1}{2}\frac{\mathcal{M}_{\rm E}}{\mathcal{M}_{\rm E}+2} < \frac{1}{2}.$$

Our next objective is to determine the conditions that maximize efficiency and the output power obtained at these points. At resonance, the efficiency is

$$\eta = \frac{R_{\rm E}}{R_1+R_{\rm E}}\frac{\Psi^2}{\Psi^2+b(R_1+R_{\rm E})}.$$

Solving equation $\mathrm{d}\eta/\,\mathrm{d}R_{\rm E}=0$, we get

$$R_{\rm E} = R_1\sqrt{1+\mathcal{M}_{\rm E}},$$

which leads to the maximum efficiency of

$$\eta = \frac{\mathcal{M}_{\rm E}}{(1+\sqrt{1+\mathcal{M}_{\rm E}})^2}. \tag{22}$$

Interestingly, the same expression of highest efficiency has been observed in other energy harvesting and wireless power transfer architectures, including resonant inductive (capacitive) coupled and magnetoelectric–based systems, with the respective figure of merits [42], [43]. The output power under these conditions is

$$P_{\rm E}|_{\max\{\eta\}} = \frac{F_0^2}{2b}\frac{\mathcal{M}_{\rm E}}{(1+\sqrt{1+\mathcal{M}_{\rm E}})^2}\frac{1}{\sqrt{1+\mathcal{M}_{\rm E}}}. \tag{23}$$

The ratio between the power in (8) and (23) is then

$$\frac{\max\{P_{\rm E}\}}{P_{\rm E}|_{\max\{\eta\}}} = \frac{\left(1+\sqrt{1+\mathcal{M}_{\rm E}}\right)^2}{4\sqrt{1+\mathcal{M}_{\rm E}}} > 1\,\forall \mathcal{M}_{\rm E}>0.$$

Therefore, when the efficiency is optimized, the output power is always less than its maximum value. We note that the maximum power (8) and the optimal efficiency (22) share the same trend, in which they increase with $\mathcal{M}_{\rm E}$. However, and more importantly, the power at the maximum efficiency point in (23) does not follow this trend. It first increases and reaches its maximum of $(3/2-\sqrt{2})F_0^2/b$ at $\mathcal{M}_{\rm E}=2(1+\sqrt{2})$, and then decreases with $\mathcal{M}_{\rm E}$. At the limit, $\lim_{\mathcal{M}_{\rm E}\to+\infty} P_{\rm E}|_{\max\{\eta\}}=0$ and $\lim_{\mathcal{M}_{\rm E}\to+\infty}\eta=1$, which is in line with the results in Section VII-A.

C. Hybrid energy harvesting system

At resonance, the input and total output power and efficiency of the piezoelectric–electromagnetic hybrid system are derived as follows

$$P_{\rm in} = \frac{1}{2}\frac{F_0^2}{\Re\{Z_{\rm in}\}},$$
$$P_{\rm T} = \frac{1}{2}\frac{F_0^2}{\Re\{Z_{\rm in}\}^2}\left[\frac{\Psi^2 R_{\rm E}}{(R_{\rm E}+R_1)^2}+\frac{\Gamma^2 R_0^2 R_{\rm P}}{(R_0+R_{\rm P})^2}\right],$$
$$\eta = \frac{P_{\rm T}}{P_{\rm in}} = \frac{1}{\Re\{Z_{\rm in}\}}\left[\frac{\Psi^2 R_{\rm E}}{(R_{\rm E}+R_1)^2}+\frac{\Gamma^2 R_0^2 R_{\rm P}}{(R_0+R_{\rm P})^2}\right]$$

where the imaginary part of the input impedance vanishes and the real part is

$$\Re\{Z_{\rm in}\} = b+\Psi^2/(R_1+R_{\rm E})+\Gamma^2\left(R_0^{-1}+R_{\rm P}^{-1}\right)^{-1}.$$

We can write these expressions in terms of time scales and effective figures of merit as

$$P_{\rm T} = \frac{1}{2}\frac{F_0^2 b}{\Re\{Z_{\rm in}\}^2}\left[\mathcal{M}_{\rm E}\frac{\tau_1/\tau_{\rm E}}{(1+\tau_1/\tau_{\rm E})^2}+\mathcal{M}_{\rm P}\frac{\tau_{\rm P}/\tau_0}{(1+\tau_{\rm P}/\tau_0)^2}\right],$$
$$\eta = \frac{b}{\Re\{Z_{\rm in}\}}\left[\mathcal{M}_{\rm E}\frac{\tau_1/\tau_{\rm E}}{(1+\tau_1/\tau_{\rm E})^2}+\mathcal{M}_{\rm P}\frac{\tau_{\rm P}/\tau_0}{(1+\tau_{\rm P}/\tau_0)^2}\right],$$
$$\Re\{Z_{\rm in}\} = b\left(1+\frac{\mathcal{M}_{\rm E}}{1+\tau_1/\tau_{\rm E}}+\mathcal{M}_{\rm P}\frac{\tau_{\rm P}/\tau_0}{1+\tau_{\rm P}/\tau_0}\right), \tag{24}$$

which are used to study the output power and system efficiency in the following analysis.

We first consider the optimal power conditions. Substituting (12) and (13) into (24), we recover the maximum output power in (17). The input power and the efficiency at maximum power point take on the forms

$$P_{\rm in} = \frac{F_0^2}{4b}\frac{\mathcal{M}_{\rm E}+\mathcal{M}_{\rm P}+2}{\sqrt{\mathcal{M}_{\rm E}+1}\sqrt{\mathcal{M}_{\rm P}+1}\sqrt{\mathcal{M}_{\rm E}+\mathcal{M}_{\rm E}+1}},$$
$$\eta|_{\max\{P_{\rm T}\}} = \left(\frac{1}{\mathcal{M}_{\rm E}}+\frac{1}{\mathcal{M}_{\rm P}}\right)\frac{(\mathcal{M}_{\rm E}+1)(\mathcal{M}_{\rm P}+1)-\sqrt{(\mathcal{M}_{\rm E}+1)(\mathcal{M}_{\rm P}+1)(\mathcal{M}_{\rm E}+\mathcal{M}_{\rm P}+1)}}{\mathcal{M}_{\rm E}+\mathcal{M}_{\rm P}+2}.$$

When only one transduction mechanism (either piezoelectric or electromagnetic) is active $\eta|_{\max\{P_{\rm T}\}}$ simplifies to the corresponding expression in Section VII-B,

$$\lim_{\mathcal{M}_{\rm P}\to 0}\eta|_{\max\{P_{\rm T}\}} = \frac{1}{2}\frac{\mathcal{M}_{\rm E}}{\mathcal{M}_{\rm E}+2},$$
$$\lim_{\mathcal{M}_{\rm E}\to 0}\eta|_{\max\{P_{\rm T}\}} = \frac{1}{2}\frac{\mathcal{M}_{\rm P}}{\mathcal{M}_{\rm P}+2},$$

showing the consistency between the single– and multiple–mechanism models.

Our next aim is to determine the optimal efficiency and the according output power at the same conditions. The stationary points of the efficiency η in (24) can be found by solving equations $\mathrm{d}\eta/R_{\rm E}=0$ and $\mathrm{d}\eta/R_{\rm P}=0$ simultaneously, which result in

$$R_{\rm E} = R_1\sqrt{\mathcal{M}_{\rm E}+\mathcal{M}_{\rm P}+1},$$
$$R_{\rm P} = R_0/\sqrt{\mathcal{M}_{\rm E}+\mathcal{M}_{\rm P}+1}.$$

The maximum efficiency is then

$$\eta = 1-2\frac{\sqrt{\mathcal{M}_{\rm E}+\mathcal{M}_{\rm P}+1}-1}{\mathcal{M}_{\rm E}+\mathcal{M}_{\rm P}}, \tag{25}$$

with the corresponding power

$$P_{\rm T}|_{\max\{\eta\}} = \frac{F_0^2}{2b}\left[\frac{2+\mathcal{M}_{\rm E}+\mathcal{M}_{\rm P}}{(\mathcal{M}_{\rm E}+\mathcal{M}_{\rm P})\sqrt{\mathcal{M}_{\rm E}+\mathcal{M}_{\rm P}+1}}-\frac{2}{\mathcal{M}_{\rm E}+\mathcal{M}_{\rm P}}\right]. \tag{26}$$

When $\mathcal{M}_\mathrm{P} \to 0$, equations (25) and (26) reduce to (22) and (23), respectively. This further underscores the coherence between the two models.

Taking the ratio between the power in (17) and (26) and algebraically simplifying, it follows that

$$\frac{\max\{P_\mathrm{T}\}}{P_\mathrm{T}|_{\max\{\eta\}}} = \frac{\left(\sqrt{\mathcal{M}_\mathrm{E}+\mathcal{M}_\mathrm{P}+1}+1\right)^2}{2\left(\sqrt{\mathcal{M}_\mathrm{E}+1}\sqrt{\mathcal{M}_\mathrm{P}+1}+\sqrt{\mathcal{M}_\mathrm{E}+\mathcal{M}_\mathrm{P}+1}\right)} = \frac{(\mathcal{M}_\mathrm{E}+1)+(\mathcal{M}_\mathrm{P}+1)+2\sqrt{\mathcal{M}_\mathrm{E}+\mathcal{M}_\mathrm{P}+1}}{2\sqrt{\mathcal{M}_\mathrm{E}+1}\sqrt{\mathcal{M}_\mathrm{P}+1}+2\sqrt{\mathcal{M}_\mathrm{E}+\mathcal{M}_\mathrm{P}+1}}.$$

Due to the Cauchy–Schwarz inequality, $(\mathcal{M}_\mathrm{E}+1)+(\mathcal{M}_\mathrm{P}+1) \geq 2\sqrt{\mathcal{M}_\mathrm{E}+1}\sqrt{\mathcal{M}_\mathrm{P}+1}$ for all positive $\mathcal{M}_\mathrm{E}$ and $\mathcal{M}_\mathrm{P}$. As a consequence, this power ratio is always equal or greater than unity. The equality holds if and only if $\mathcal{M}_\mathrm{E} = \mathcal{M}_\mathrm{P}$. Therefore, if the two transducers have the same effective figure of merit, optimizing efficiency can be considered as equivalent to maximizing the total output power. This is a *distinctive property of a hybrid energy harvesting system* that is not observed in the single–mechanism generators (i.e., in this case, the power ratio is strictly less than unity, and equality can never take place). However, in most regions of the parameter spaces of $\mathcal{M}_\mathrm{E}$ and $\mathcal{M}_\mathrm{P}$, optimizing efficiency results in a lower power compared to directly maximizing the output power.

With all the findings revealed in Section VII, we strive to provide a comprehensive assessment of the performance of three models, namely electrically–lossless transducer, and single–mechanism and hybrid generators, in terms of power and efficiency. In most cases of resonant and displacement–unconstrained energy harvesting, optimizing efficiency and maximizing power should be treated as separate problems since they generally yield different global solutions. However, there are specific scenarios in a hybrid structure where the two objectives have a unique solution, and this manifests when the effective figures of merit of the two resonators are equal. For the models under consideration, choosing output power as the primary metric for optimization is naturally appropriate.

The performance of single-mechanism and hybrid energy harvesting systems in this study is compared primarily in terms of power and efficiency. However, it should be noted that a hybrid configuration, which combines piezoelectric or triboelectric and electromagnetic transducers, holds the potential to offer benefits in terms of operation bandwidth and can provide a broader design space for a power electronic interface [44], [45].

The feasibility of a hybrid system integrating piezoelectric and electromagnetic generators within a small–scale hybrid system, such as MEMS/NEMS devices, remains uncertain due to the difference in scaling laws [46]. Under constant input acceleration, the maximum output power of a piezoelectric harvester scales with the fourth power of the scaling factor L_s, and it scales with the seventh power for an electromagnetic generator [47], [48]. Here, $L_\mathrm{s} = \sqrt[3]{V_\mathrm{a}}$, where V_a is the active volume. These relationships also imply that, as devices decrease in size, the output voltage of the electromagnetic harvester reduces at a much faster rate compared to that of the piezoelectric generator. Consequently, voltage rectification becomes more challenging. Furthermore, electromagnetic harvesters usually consist of discrete components, which poses difficulties for integration at a smaller scale. However, these concerns are beyond the scope of the paper, and we leave them open for future consideration.

VIII. Conclusion

We have shown that it is unnecessary to utilize a hybrid configuration for idealized two–port harvesters with electrical losses neglected. When these parasitic losses are accounted for, we have derived analytical expressions for the maximum output power that an energy harvesting system can provide for two cases, when using only one transduction mechanism and a hybrid system with piezoelectric and electromagnetic transducers. We have identified the conditions between effective figures of merit of the electromagnetic and piezoelectric transductions $\mathcal{M}_\mathrm{E}$ and $\mathcal{M}_\mathrm{P}$, under which one system yields more benefits than the other in terms of power. In a broader space of these two quantities, a hybrid system is not beneficial and can even cause a decrease in the maximum output power if either the piezoelectric or electromagnetic transducer has an effective figure of merit above a threshold value of $\mathcal{M}^* \approx 2.17$. A thorough investigation shows that optimizing system efficiency generally leads to a power that is lower than the maximum obtainable power. Optimizing efficiency and maximizing power resulting in a unique solution only occurs in a hybrid structure and when both transductions have the same effective figure of merit. These findings could provide valuable insights for the design of efficient energy harvesting systems. All results apply to linear vibration energy harvesters, with linear mechanical stiffness, linear energy conversion, and linear loading, under harmonic excitation.

Appendix A
An Alternative Approach to Determining the Power Limit of a Single Mechanism Systems

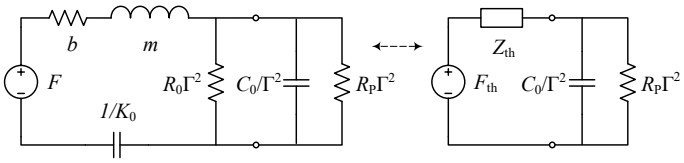

Fig. 11: Thévenin equivalent circuit.

Here we seek to find the maximum possible power delivered to the load based on the reflected impedance method and network theory, without forming a resonator in the electrical domain. Figure 11 shows Thévenin equivalent circuit of a piezoelectric energy harvester depicted in Figure 7 when the external inductor L_0 is omitted. The Thévenin equivalent voltage and impedance are given by

$$F_\mathrm{th} = F_0 \frac{R_0\Gamma^2}{\Gamma^2 R_0 + b + j\omega m + K_0/(j\omega)}, \tag{27}$$

$$Z_\mathrm{th} = \frac{R_0\Gamma^2\left(b + j\omega m + K_0/(j\omega)\right)}{R_0\Gamma^2 + b + j\omega m + K_0/(j\omega)}. \tag{28}$$

Based on the network theory, the largest possible power that can be transferred to the load is the maximum power available from the source formed by $F_{\rm th}$ and $Z_{\rm th}$, which is

$$P_{\rm P} = \max\left\{ P_{\rm avs} = \frac{|F_{\rm th}|^2}{8\Re\{Z_{\rm th}\}} \right\}.$$

From (27) and (28), we get

$$P_{\rm avs} = \frac{1}{8}\frac{F_0^2\Gamma^2 R_0}{(m\omega - K_0/\omega)^2 + b^2(\Gamma^2 R_0/b+1)}.$$

$P_{\rm avs}$ reaches its maximum when $\omega = \sqrt{K_0/m}$, and as a consequence,

$$P_{\rm P} = \frac{F_0^2}{8b}\frac{\Gamma^2 R_0/b}{\Gamma^2 R_0/b+1} = \frac{F_0^2}{8b}\frac{\mathcal{M}_{\rm P}}{\mathcal{M}_{\rm P}+1},$$

which coincides with (9).

This technique, using the network theory, is convenient to derive the upper bound of power. However, the method presented in Section IV is more comprehensive in whether it is possible and how to attain or approach the power bound.

Appendix B
Optimal Load and Frequency

Sometimes, adding an inductor or capacitor to form a resonator in the electrical domain is not convenient. We now investigate the optimal load and frequency without those elements and compare the optimum performance of the transducer to the power bound.

Taken the electromagnetic generator as an example, the stationary points of the power are determined by $\partial P/\tau_{\rm E} = 0$ and $\partial P/\omega = 0$. The former equation results in

$$\begin{aligned}\tau_{\rm E} = \tau_1\Big[(K_0 - m\omega^2)^2 + (\omega b)^2\Big]^{1/2} \Big/ \\ \Big[(K_0 - m\omega^2)^2 + (K_{\rm E} - m\omega^2)^2(\omega\tau_1)^2 \\ + (\omega b)^2(1+(\omega\tau_1)^2) + 2\Delta K_{\rm E}(\omega^2 b\tau_1)\Big]^{1/2}.\end{aligned} \tag{29}$$

The latter equation reduces to

$$2(m\tau_\alpha)^2\Omega^3 + \big(m^2 + \tau_\alpha^2(b^2 - 2mK_{\rm E})\big)\Omega^2 - K_0^2 = 0 \tag{30}$$

where $\Omega = \omega^2$ and $1/\tau_\alpha = 1/\tau_{\rm E} + 1/\tau_1$. Equations (29) and (30) are coupled and nonlinear. Therefore, using numerical methods to find their solutions are more appropriate than analytical counterparts.

A common method to approach the power bound is to operate the system at its resonance frequency and maximizing the output power by optimizing the load, resulting in

$$\tau_{\rm E} = \frac{\tau_1}{\sqrt{(\mathcal{M}_{\rm E}+1)^2 + Q_{\rm L}^2}}, \tag{31}$$

$$P_{\rm E} = \frac{F_0^2}{8b}\frac{2\mathcal{M}_{\rm E}}{\mathcal{M}_{\rm E}+1+\sqrt{(\mathcal{M}_{\rm E}+1)^2+Q_{\rm L}^2}}. \tag{32}$$

The expressions (31) and (32) simplify to (7) and (8) when $\mathcal{M}_{\rm E}+1 \gg Q_{\rm L}$.

We find that both methods – (i) simultaneously optimizing the load and frequency, and (ii) only optimizing the load while operating at the resonance frequency – result in power values that are nearly identical to each other and to the power limit. A demonstration is shown in Figure 12. We can also perform the same analysis and obtain similar results for the piezoelectric generator, except that $\tau_{\rm E}, \tau_1, \tau_\alpha, \Delta K_{\rm E}$ and $K_{\rm E}$ are now replaced by $\tau_{\rm P}, \tau_0, \tau_\beta, \Delta K_{\rm P}$ and $K_{\rm P}$, respectively, where $\tau_\beta = (1/\tau_{\rm P} + 1/\tau_0)^{-1}$.

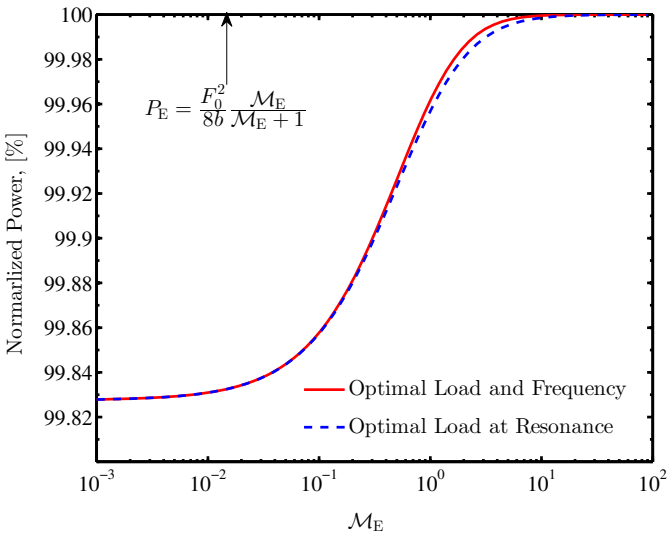

Fig. 12: Comparison of output power for single–transduction systems under different optimal conditions, (i) simultaneous optimization of the load and frequency, and (ii) optimization of the load at resonance frequency, which is made to the maximum achievable power given by equation (8).

Acknowledgment

This material is based upon work supported by the National Science Foundation under Grant No. 1651438 for author Shad Roundy and by the Research Council of Norway Grant No. 299279 for author Cuong Phu Le.

References

[1] S. Priya and D. Inman, *Energy Harvesting Technologies*. Springer US, 2008.

[2] A. Dewan, S. U. Ay, M. N. Karim, and H. Beyenal, "Alternative power sources for remote sensors: A review," *Journal of Power Sources*, vol. 245, pp. 129–143, 2014.

[3] V. Misra, A. Bozkurt, B. Calhoun, T. Jackson, J. S. Jur, J. Lach, B. Lee, J. Muth, O. Oralkan, M. Öztürk, S. Trolier-McKinstry, D. Vashaee, D. Wentzloff, and Y. Zhu, "Flexible technologies for self-powered wearable health and environmental sensing," *Proceedings of the IEEE*, vol. 103, no. 4, pp. 665–681, 2015.

[4] F. K. Shaikh and S. Zeadally, "Energy harvesting in wireless sensor networks: A comprehensive review," *Renewable and Sustainable Energy Reviews*, vol. 55, pp. 1041–1054, 2016.

[5] A. Khaligh, P. Zeng, and C. Zheng, "Kinetic energy harvesting using piezoelectric and electromagnetic technologies -state of the art," *IEEE Transactions on Industrial Electronics*, vol. 57, pp. 850–860, March 2010.

[6] F. B. E. K. e. Nicu Bizon, Naser Mahdavi Tabatabaei, *Energy Harvesting and Energy Efficiency: Technology, Methods, and Applications*. Lecture Notes in Energy 37, Springer International Publishing, 1 ed., 2017.

[7] H. Ryu, H.-J. Yoon, and S.-W. Kim, "Hybrid energy harvesters: Toward sustainable energy harvesting," *Advanced Materials*, vol. 31, no. 34, p. 1802898, 2019.

[8] H. Liu, H. Fu, L. Sun, C. Lee, and E. M. Yeatman, "Hybrid energy harvesting technology: From materials, structural design, system integration to applications," *Renewable and Sustainable Energy Reviews*, vol. 137, p. 110473, 2021.

[9] S. Beeby, R. Torah, and M. Tudor, "Kinetic energy harvesting," 2008.

[10] P. Li, S. Gao, S. Niu, H. Liu, and H. Cai, "An analysis of the coupling effect for a hybrid piezoelectric and electromagnetic energy harvester," *Smart Materials and Structures*, vol. 23, p. 065016, may 2014.

[11] R. Toyabur, M. Salauddin, H. Cho, and J. Y. Park, "A multimodal hybrid energy harvester based on piezoelectric-electromagnetic mechanisms for low-frequency ambient vibrations," *Energy Conversion and Management*, vol. 168, pp. 454–466, 2018.

[12] R. Hamid and M. R. Yuce, "A wearable energy harvester unit using piezoelectric-electromagnetic hybrid technique," *Sensors and Actuators A: Physical*, vol. 257, pp. 198–207, 2017.

[13] M. Cheng, J. Wu, X. Liang, R. Mao, H. Huang, D. Ju, Z. Hu, J. Guo, and M. Liu, "Hybrid multi-mode magneto-mechano-electric generator with enhanced magnetic field energy harvesting performance," *Sensors and Actuators A: Physical*, vol. 352, p. 114194, 2023.

[14] M. A. Halim, A. A. Rendon-Hernandez, S. E. Smith, and D. P. Arnold, "Analysis of a dual-transduction receiver for electrodynamic wireless power transfer," *IEEE Transactions on Power Electronics*, vol. 37, no. 6, pp. 7470–7479, 2022.

[15] M. S. Kwak, M. Peddigari, H. Y. Lee, Y. Min, K.-I. Park, J.-H. Kim, W.-H. Yoon, J. Ryu, S. N. Yi, J. Jang, and G.-T. Hwang, "Exceeding 50 mw rms-output magneto-mechano-electric generator by hybridizing piezoelectric and electromagnetic induction effects," *Advanced Functional Materials*, vol. 32, no. 24, p. 2112028, 2022.

[16] A. Ameye, N. Decroix, N. Garraud, P. Gasnier, and A. Badel, "Increasing the robustness of electrodynamic wireless power receivers with hybrid transduction," in *2022 Wireless Power Week (WPW)*, pp. 146–150, 2022.

[17] H. A. C. Tilmans, "Equivalent circuit representation of electromechanical transducers: I. lumped-parameter systems," *Journal of Micromechanics and Microengineering*, vol. 6, pp. 157–176, 1996.

[18] Y. Liao and J. Liang, "Maximum power, optimal load, and impedance analysis of piezoelectric vibration energy harvesters," *Smart Materials and Structures*, vol. 27, p. 075053, jun 2018.

[19] P. D. Mitcheson, T. C. Green, E. M. Yeatman, and A. S. Holmes, "Architectures for vibration-driven micropower generators," *Journal of Microelectromechanical Systems*, vol. 13, pp. 429–440, June 2004.

[20] J. M. Renno, M. F. Daqaq, and D. J. Inman, "On the optimal energy harvesting from a vibration source," *Journal of Sound and Vibration*, vol. 320, no. 1, pp. 386–405, 2009.

[21] E. Halvorsen, "Optimal Load and Stiffness for Displacement-Constrained Vibration Energy Harvesters," *ArXiv e-prints*, Mar. 2016.

[22] B. D. Truong, "Power optimization of a magnetoelectric wireless power transfer system with volume constraint," *Sensors and Actuators A: Physical*, vol. 341, p. 113226, 2022.

[23] S. J. Orfanidis, *Electromagnetic Waves and Antennas*. ECE Department, Rutgers University, Online ed., 2016.

[24] C. S. Kong, "A general maximum power transfer theorem," *IEEE Transactions on Education*, vol. 38, pp. 296–298, Aug 1995.

[25] B. D. Truong, S. Williams, and S. Roundy, "Experimentally validated model and analytical investigations on power optimization for piezoelectric-based wireless power transfer systems," *Journal of Intelligent Material Systems and Structures*, vol. 30, no. 16, pp. 2464–2477, 2019.

[26] F. Goldschmidtboeing, M. Wischke, C. Eichhorn, and P. Woias, "Parameter identification for resonant piezoelectric energy harvesters in the low- and high-coupling regimes," *Journal of Micromechanics and Microengineering*, vol. 21, p. 045006, mar 2011.

[27] M. Renaud, R. Elfrink, M. Jambunathan, C. de Nooijer, Z. Wang, M. Rovers, R. Vullers, and R. van Schaijk, "Optimum power and efficiency of piezoelectric vibration energy harvesters with sinusoidal and random vibrations," *Journal of Micromechanics and Microengineering*, vol. 22, no. 10, p. 105030, 2012.

[28] A. Morel, A. Badel, R. Grázaud, P. Gasnier, G. Despesse, and G. Pillonnet, "Resistive and reactive loads' influences on highly coupled piezoelectric generators for wideband vibrations energy harvesting," *Journal of Intelligent Material Systems and Structures*, vol. 30, no. 3, pp. 386–399, 2019.

[29] A. Brenes, A. Morel, J. Juillard, E. Lefeuvre, and A. Badel, "Maximum power point of piezoelectric energy harvesters: a review of optimality condition for electrical tuning," *Smart Materials and Structures*, vol. 29, p. 033001, jan 2020.

[30] D. Gibus, A. Morel, P. Gasnier, A. Ameye, and A. Badel, "High performance piezoelectric vibration energy harvesting by electrical resonant frequency tuning," *Smart Materials and Structures*, vol. 31, p. 125012, nov 2022.

[31] H. Wheeler, "Simple inductance formulas for radio coils," *Proceedings of the Institute of Radio Engineers*, vol. 16, pp. 1398–1400, Oct 1928.

[32] S. Cheng, N. Wang, and D. P. Arnold, "Modeling of magnetic vibrational energy harvesters using equivalent circuit representations," *Journal of Micromechanics and Microengineering*, vol. 17, p. 2328, oct 2007.

[33] M. Wild, M. Bring, E. Halvorsen, L. Hoff, and K. Hjelmervik, "The challenge of distinguishing mechanical, electrical and piezoelectric losses," *The Journal of the Acoustical Society of America*, vol. 144, pp. 2128–2134, 10 2018.

[34] Z. Yang, S. Zhou, J. Zu, and D. Inman, "High-performance piezoelectric energy harvesters and their applications," *Joule*, vol. 2, no. 4, pp. 642–697, 2018.

[35] A. Badel and E. Lefeuvre, *Nonlinear Conditioning Circuits for Piezoelectric Energy Harvesters*, pp. 321–359. Cham: Springer International Publishing, 2016.

[36] E. Lefeuvre, A. Badel, A. Brenes, S. Seok, M. Woytasik, and C.-S. Yoo, "Analysis of piezoelectric energy harvesting system with tunable sece interface," *Smart Materials and Structures*, vol. 26, p. 035065, feb 2017.

[37] C. D. Richards, M. J. Anderson, D. F. Bahr, and R. F. Richards, "Efficiency of energy conversion for devices containing a piezoelectric component," *Journal of Micromechanics and Microengineering*, vol. 14, no. 5, pp. 717–721, 2004.

[38] S. Roundy, "On the effectiveness of vibration-based energy harvesting," *Journal of Intelligent Material Systems and Structures*, vol. 16, no. 10, pp. 809–823, 2005.

[39] Y. C. Shu and I. C. Lien, "Analysis of power output for piezoelectric energy harvesting systems," *Smart Materials and Structures*, vol. 15, pp. 1499–1512, 2006.

[40] M. Kim, J. Dugundji, and B. L. Wardle, "Efficiency of piezoelectric mechanical vibration energy harvesting," *Smart Materials and Structures*, vol. 24, p. 055006, apr 2015.

[41] T. W. Blad and N. Tolou, "On the efficiency of energy harvesters: A classification of dynamics in miniaturized generators under low-frequency excitation," *Journal of Intelligent Material Systems and Structures*, vol. 30, no. 16, pp. 2436–2446, 2019.

[42] B. D. Truong, T. T.-T. Le, and B. Sensale-Rodriguez, "Two-coil wireless power transfer system configured in series-series topology: Fundamental dynamics and limitations on transmitted power," 2020.

[43] E. Andersen, S. Roundy, and B. D. Truong, "Frequency–dependence of power and efficiency for resonant inductive coupling and magnetoelectric wireless power transfer systems," *Smart Materials and Structures*, vol. 31, p. 105026, sep 2022.

[44] G. Lombardi and M. Lallart, "Synchronous electric charge and induced current extraction (secice): a unified nonlinear technique combining piezoelectric and electromagnetic harvesting," *Smart Materials and Structures*, vol. 30, p. 025029, jan 2021.

[45] S. Naval, N. T. Beigh, A. Jain, and D. Mallick, "Bandwidth tunable vibration energy harvester based on hybrid triboelectric-piezoelectric array," *Engineering Research Express*, vol. 4, p. 045022, nov 2022.

[46] P. Gardonio and L. Dal Bo, "Scaling laws of electromagnetic and piezoelectric seismic vibration energy harvesters built from discrete components," *Journal of Sound and Vibration*, vol. 476, p. 115290, 2020.

[47] C. Zhu, V. C. M. Leung, L. Shu, and E. C. H. Ngai, "Green internet of things for smart world," *IEEE Access*, vol. 3, pp. 2151–2162, 2015.

[48] S. D. Moss, O. R. Payne, G. A. Hart, and C. Ung, "Scaling and power density metrics of electromagnetic vibration energy harvesting devices," *Smart Materials and Structures*, vol. 24, no. 2, p. 023001, 2015.